LUMEN ET VIRTUS

Use of ultrasound for analysis of the properties of a copper-plated grounding rod

https://doi.org/10.56238/levv15n39-183

Álvaro Barbosa de Carvalho Júnior[1], Ana Cristina Vieira Amaral[2], Maurílio José Inácio[3], Adalto Soares da Fonseca Júnior[4], Maria Helena Teles Lopes[5] and Vera Lúcia Alves[6]

ABSTRACT

The main objective of this work was to use ultrasonic wave values and density to analyze the elastic and physical properties of a copper-plated rod used for grounding. For this, an electronic ultrasound system with 2 MHz piezoelectric transducers and mathematical models that are a function of the propagation speeds of the ultrasonic waves was used. The ultrasonic speeds were determined with the transmission method using petroleum jelly paste as the couplant material. Thus, through the specific equations for isotropic materials, it was possible to estimate some elastic properties, such as modulus of elasticity, shear and compressibility, Poisson coefficient and anisotropy factor, in addition to the physical property of acoustic impedance. The properties of the grounding rod were evaluated before and after a chemical attack with nitric acid to remove the copper layer. As a result, the feasibility of using ultrasound as a non-destructive technique, capable of detecting small changes in the properties of the nail after chemical attack, was verified. The results were compared with the electrical resistivity test and discussed as a function of the values of physical and mechanical properties reported in the literature for the grounding rods.

Keywords: Ultrasonic Waves, Copper, Bar, Grounding.

[1] E-mail: alvaro.junior@unimontes.br
[2] E-mail: cristinaamaral859@gmail.com
[3] E-mail: maurilio.inacio@unimontes.br
[4] E-mail: adalto.junior@unimontes.br
[5] E-mail: mariahelenatl23@gmail.com
[6] E-mail: vera.alves@unimontes.br

INTRODUCTION

It is known that in buildings, grounding provides not only the stability and safety of the electrical installation, but also the safety of its users. This is because the main function of grounding is to place the installations at the same electrical potential, keeping the difference in electrical potential between the earth and the equipment close to zero (ABNT NBR 5410:2008).

It is known that residential electrical grounding can be done with the use of rods manufactured from drawn steel core with electrolytic copper coating. These characteristics favor greater resistance and mechanical rigidity, allowing the rods to be driven into the ground without the need for previous holes. The copper-coated steel rod behaves mechanically as a single metal, whose copper coating eliminates the possibility of corrosion of the steel (ABNT NBR 5410:2008). In addition, the pointed end of the rod is cold worked, increasing the hardness and toughness of the rod

Grounding rods can be defined as a grounding electrode, which consists of a rigid cylindrical bar of copper-coated steel by electroplating. In addition, some requirements are also found for the use of rods and their accessories, such as grounding connector and splice sleeve, which must be produced with materials that withstand the electrical, mechanical, and chemical conditions, from the different installation locations (ABNT NBR 13571:2024).

The mechanical properties of steels used as rod cores are generally determined with conventional destructive tests, among which tensile, compression, shear and bending tests stand out. Some authors report that these tests require time and cost with the preparation of several samples that will be rendered useless due to rupture or damage, with no possibility of repeating measurements (CARVALHO JR et al., 2022; LOPES et al., 2024). In addition, for a more comprehensive mechanical characterization, it is necessary to carry out several types of mechanical tests.

On the other hand, ultrasonic testing emerges as a viable alternative that allows the estimation of various properties of steel without the need to destroy or damage it. This possibility results in lower time and cost compared to conventional destructive testing (CARVALHO JR et al., 2021; CARVALHO JR et al., 2022; LOPES et al., 2024). It is important to highlight that the advantage of using ultrasound for steel characterization consists in the calculation of properties by means of mathematical models that are described as a function of density and longitudinal and transverse ultrasonic wave propagation velocity values (ASTM E494-95, 1995; ERAIAH; GEETHA; ANAVEKAR, 2008).

Although it is known that ultrasonic testing is used by many large companies, it is believed that due to the lack of knowledge of ultrasonic techniques and the consolidation of conventional destructive testing, many medium and small companies do not use ultrasonic testing to characterize their steel products. Therefore, this work aimed to use the ultrasonic test to calculate the elastic and

physical properties of a copper-coated steel grounding rod, which was subjected to a chemical attack with nitric acid for comparative analysis between the results.

MATERIALS AND METHODS

CHARACTERISTICS OF THE SAMPLES

To carry out this study, a common rod for electrical grounding was commercially acquired. According to the manufacturer's specification, it is a rod with a core in SAE 1020 carbon steel, coated with a minimum layer of 0.254 millimeters of high purity electrolytic copper (99.9%) without traces of zinc. The rod, whose dimensions were 2.40 meters long and 12.20 mm in diameter, was cut with the aid of a circular saw and diamond disc into three smaller bars with lengths of 0.20 m. Figure 2.1 shows the grounding rod and the samples of cut bars.

Figure 2.1 - Grounding rod and bar samples

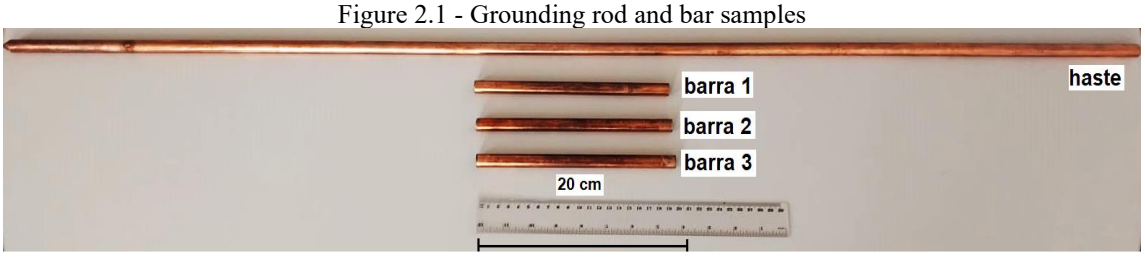

Source: authors (2024)

The density () of the bars was calculated with Equation 2.1, which consists of the ratio between mass and volume. For this, the effective dimensions were obtained with the aid of a digital caliper, and the volume was calculated using Equation 2.2. To estimate the mass, an analytical balance with a resolution of 0.001 g was used. ρ

$$\rho = \frac{m}{Vol} \qquad (2.1)$$

$$Vol = \pi . \frac{d^2}{4} . c \qquad (2.2)$$

Where:

ρ = densidade (kg/m3);

m = massa (kg);

Vol = volume (m3);

d = bar diameter (m);

c = Bar length (m).

In this study, constant inertia values attributed to circular cross-section and homogeneous mass distribution along the length of the bars were considered for the calculation of the bar density with Equation 2.1.

DETERMINATION OF ULTRASONIC VELOCITIES

To calculate the velocities of the ultrasonic waves propagated through the bars, the travel times of the longitudinal waves were measured with an electronic ultrasound system previously used in steels by the authors Carvalho Jr et al. (2021), Carvalho Jr et al. (2022) and Lopes et al. (2024). The electronic system for determining the longitudinal ultrasonic velocity (*VL)* with the transmission method is shown in Figure 2.2. In the transmission method, ultrasonic wave transducers are aligned at the ends of the bars for measurements. The material used as a couplant between the transducers and the ends of the bars was petroleum jelly paste.

Figure 2.2 - Electronic system for ultrasonic testing

Source: authors (2024)

The emitter and receiver circuits were fed with symmetrical sources of 30 V and 12 V, respectively. In the emitting circuit, pulses with an amplitude of 60 V were produced with a duration of 400 ns (nanoseconds), at time intervals of 5 ms (milliseconds). The pulses were produced with a piezoelectric longitudinal wave generator transducer, model AW190, with a diameter of 2 cm, a frequency of 2 MHz. These descriptions can be found in more detail in the study of steel 1020 carried out by Carvalho Jr. et al. (2021).

To receive the signals, another piezoelectric transducer of the same model and frequency was used. To amplify the signal received in the receiver circuit, an operational amplifier, model THS4271D, was used, designed to work with supply voltage values between ± 5 V and ± 15 V. An illustrative image of the electronic circuits emitting and receiving ultrasound is shown in Figure 2.3.

Figure 2.3 - Ultrasound electronic circuits: (a) emitter; (b) Receiver

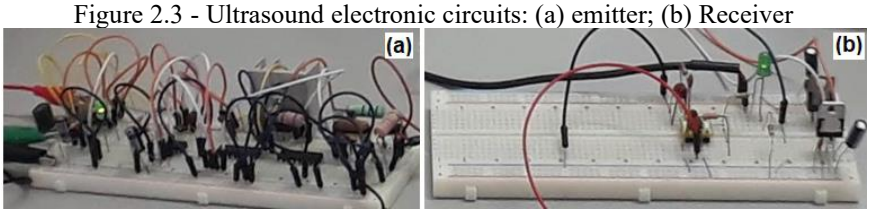

Source: authors (2024)

The measurements of the signals provided at the output of the receiver circuit were observed directly on the screen of the digital oscilloscope, Tektronix, model TBS1062. The oscilloscope connected to the computer made it possible to export the data and capture the images of the signals with the OpenChoice Desktop program. Thus, it was possible to determine the time measurement in microseconds (µs) between the ultrasonic signal emitted and received through the bars. An example of the time measurement is illustrated in Figure 2.4. The distance between the vertical lines was used to estimate the average time spent by the ultrasonic wave, calculated with three measurements performed with the removal and repositioning of the transducers on the bars.

Figure 2.4 - Determination of the ultrasonic wave travel time

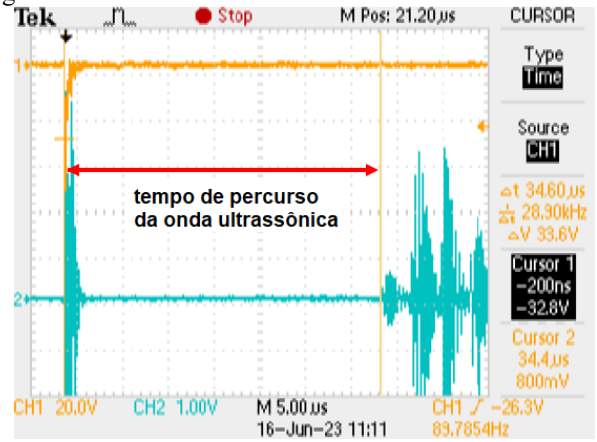

Source: authors (2024)

To calculate the average velocity of longitudinal wave propagation (*VL),* based on three time measurements, the relationship proposed in Equation 2.3 was used, which consists of the ratio between the length of the bar and the estimated propagation time of the ultrasonic wave.

$$V_L = \frac{c}{t} \qquad (2.3)$$

Where:

V_L = longitudinal ultrasonic wave velocity (m/s);

c = length of the bar (m);

t = travel time (s).

Some authors report that the ratio between transverse (*VL)* and longitudinal (*VT) ultrasonic velocities* is approximately 0.55 in carbon steel (KRAUTKRAMER; KRAUTKRAMER, 1990, p. 14). This relationship was also successfully used by Waag, Hoff and Norli (2012) for the determination of transverse ultrasonic velocity in stainless steel. Therefore, to estimate the VT value, Equation 2.4 was used, obtained from the reference values shown in Table 2.1 for 1020 steel.

$$V_T = 0{,}55V_L \qquad (2.4)$$

Table 2.1 - Reference values for 1020 steel

References	*VL* (*m/s*)	*VT* (*m/s*)	*VT/VL*
Gur e Keles (2003, p. 617)	5.899	3.237	0,549
Olympus (2019, p. 48)	5.890	3.240	0,550

Source: authors (2024)

ESTIMATION OF ELASTIC AND PHYSICAL PROPERTIES

It is known that many elastic and physical properties of isotropic materials can be expressed as a function of the density and values of the propagation velocities of ultrasonic waves. Among the properties that can be calculated for isotropic materials, such as glass and steel, the following stand out: modulus of elasticity (*E*), shear (*G*) and compressibility (*B*); acoustic impedance (*Z*), Poisson coefficient (*v*) and anisotropy factor () (ASTM-E494-95, 1995; BUDI; HUSSIN; SAHAR, 2002; ALAZOUMI et al., 2017; PALANI; SELVARASI, 2017). These properties can be calculated using A_0 *VL, VT* and values as shown in the equations for isotropic materials in Table 2.2. ρ

Table 2.2 - Equations for the calculation of properties

Property	Unit	Equation
$E = \rho V_T^2 \left(\frac{3V_L^2 - 4V_T^2}{V_L^2 - V_T^2}\right)$	GPa	(2.5)
$G = \rho V_T^2$	GPa	(2.6)
$B = \rho \left(V_L^2 - \frac{4V_T^2}{3}\right)$	GPa	(2.7)
$Z = \rho V_L$	106 kg/m2s	(2.8)
$v = \frac{(V_L^2 - 2V_T^2)}{2(V_L^2 - V_T^2)}$	-	(2.9)
$A_0 = 3^{1/2} \left(\frac{V_T^2}{V_L^2}\right)^{1/2}$	-	(2.10)

Source: authors (2024)

According to the ASTM-E494-95 (1995) standard, ultrasonic velocity measurements are very useful for the calculation of important properties of materials, highlighting some advantages in the use of equations for isotropic materials, such as: (a) it does not damage the sample; (b) results are similar to destructive testing; (c) repeatability of measurements; (d) possibility of use in different types of materials; (e) possibility of fault detection; (f) speed of results; (g) existence of portable equipment. These characteristics are among the motivations for the use of ultrasound as a non-destructive methodology for grounding rod investigation.

DETERMINATION OF THE STATIC MODULUS OF ELASTICITY

To calculate the static modulus of elasticity of the coppered nail, a three-point flexure test adapted from the procedures described by Garcia, Spim and Santos (2012, p. 173) was performed. The flexion of the shaft was caused with a dumbbell with a mass equal to 2.921 kg (28.626 N), which was installed in the middle of the length of the shaft. The useful length of the rod installed between two vertical supports was 1,150 m. To calculate the deflection caused by the dumbbell, a laser tape measure was positioned at the midpoint of the rod. The deflection was determined by means of the difference between the values observed on the tape measure, before and after the positioning of the dumbbell at half the useful length. This procedure was repeated three times to calculate the mean deflection. Figure 2.5 illustrates the adapted three-point flexure test.

Figure 2.5 - Representative scheme of the three-point flexure test

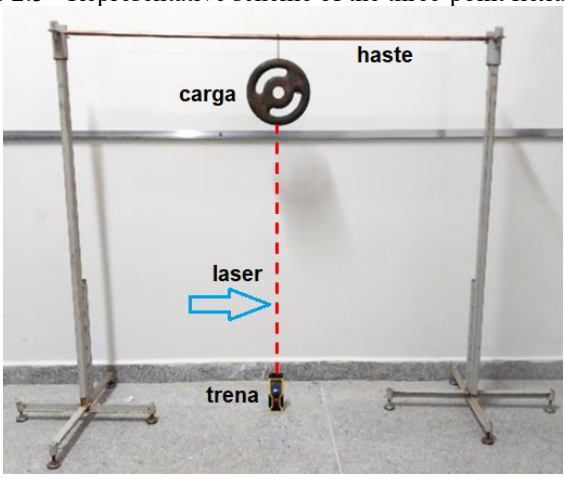

Source: authors (2024)

According to Garcia, Spim and Santos (2012, p. 186), the deflection caused by a load concentrated in the middle of the useful length can be determined by means of Equation 2.11. This equation can be reformulated and used to determine the static modulus of elasticity, as can be observed by Equations 2.12 and 2.13.

$$\Delta = \frac{P.L^3}{48.E.I} \quad (2.11)$$

$$E = \frac{P.L^3}{48.I.v} \quad (2.12)$$

$$I = \frac{\pi.d^4}{64} \quad (2.13)$$

Where:

Δ = stem deflection (mm);

P = load from the dumbbell mass (N);

L = usable length between supports (mm);

E = static modulus of elasticity (N/mm2 or MPa);

I = moment of inertia of the circular section (mm4);

d = rod diameter (mm).

CHEMICAL ATTACK OF THE BARS

To perform the chemical attack, the bar samples were dipped in a container containing a nitric acid (HNO3) solution with a concentration content of 65% B.A., as illustrated in Figure 2.6(a). The bars remained dipped in periods of 24, 48 and 144 hours. The chemical attack promotes an exothermic reaction with rapid dissolution, in which the copper layer reacts with nitric acid to form copper(II) nitrate ($Cu(NO3)_2$), subsequently releasing nitrogen oxide (NO2) and water (H2O). Generally, the formation of $Cu(NO3)_2$ is indicated by the presence of a greenish coloration, as illustrated in the image in Figure 2.6(b).

Figure 2.6 – Images of the bars: (a) before and (b) after the chemical attack

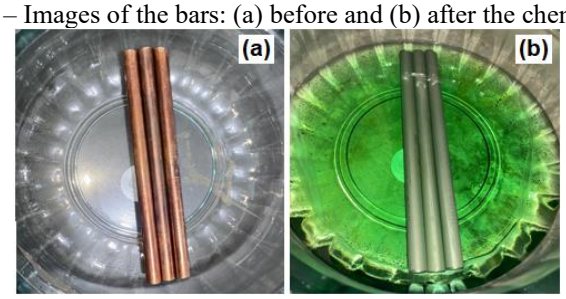

Source: authors (2024)

The chemical attack was carried out in order to analyze the influence of the copper layer on the elastic and physical properties of the bars investigated with ultrasound and electrical resistivity tests, which in this work will be represented by *R*. The resistivity test was performed at room temperature of 20.3 ± 1.0 °C and relative humidity of 49.0 ± 5.0%. The instrumentation used for the

electrical measurements was a Digital Multimeter, from the MINIPA brand, and a Standard Resistive Decade, from the INSTRUTEMP brand. The experimental results of *R* were obtained at the Measurement Laboratory of the Company MSMI - Integrated Metrological Measurements.

RESULTS AND DISCUSSION

SAMPLE DENSITY

The calculated density results for the bars are presented in Table 3.1. Before the chemical attack, the average density of the bars was 7,898 ± 16 kg/m³. The value adopted as the density of 1020 steel is 7,860 kg/m3 (EUN, 2020, p. 329). However, this value can vary between 7,840 and 7,870 kg/m3, due to the different processes used to obtain this type of steel (FREITAS et al., 2010; MEZA; FRANK; EALO, 2019). On the other hand, Callister Jr., (2012, p. 640) reports that the density of high-purity electrolytic copper is 8,890 kg/m3. This may explain why the density of the copper bar, which consists of copper-clad 1020 steel, has a higher value than the density of 1020 steel.

Table 3.1 - Density of bars before and after chemical attack

Before the chemical attack			
Mass (kg)	Volume (10-5m3)	ρ (kg/m3)	
0.18635 ± 0.00034	2.35933 ± 0.00883	7,898 ± 16	
After chemical attack			
Time (h)	Mass (kg)	Volume (10-5m3)	ρ (kg/m3)
24	0.18541 ± 0.00039	2,34966 ± 0,00914	7.891 ± 14
48	0,18530 ± 0,00027	2,35039 ± 0,00430	7,884 ± 8
144	0,18520 ± 0,00034	2,35748 ± 0,00692	7.856 ± 9

Source: authors (2024)

The density of the bars decreases with the time of residence in HNO3 solution. This occurs due to the removal of the copper layer as a function of the time of chemical attack. The copper layer was completely removed after 144 hours of chemical attack, reducing the density from 7,898 ± 16 kg/m3 to 7,856 ± 9 kg/m3. This result is close to the value adopted for the density of steel 1020 (= 7,860 kg/mρ^3), reinforcing the influence of the copper layer on the density of the bars.

ULTRASONIC SPEEDS ON THE BARS

Table 3.2 presents the results calculated for the ultrasonic speeds. In bars 1 and 2 the results were the same, namely: *VL* = 5,872 m/s and *VT* = 3,230 m/s. However, in bar 3 lower results were obtained, with *VL* = 5,838 m/s and *VT* = 3,211 m/s.

Table 3.2 – Results of *VL* and *VT* for copper bars

Bar	Length (m)	Time (10-6 s)	*VL* (m/s)	*VT* = 0,55VL (m/s)
1	0,202	34,40	5.872	3.230
2	0,202	34,40	5.872	3.230
3	0,202	34,60	5.838	3.211
Average	0,202	34.47 ± 0.12	5,861 ± 20	3,224 ± 11

Source: authors (2024)

An explanation for the longer time found in bar 3 can be found by analyzing the faces of the bar ends (Figure 3.1). The ends used for the positioning of the transmitter and receiver transducers are illustrated in Figures 3.1(a) and (b), respectively. Comparing the ends of bars 1 and 2, it is noted the presence of the 1020 carbon steel core coated by a small outer layer of copper. On the other hand, on the face of the end used to receive the ultrasonic signal in bar 3, a layer of copper is perceived, and it is not possible to clearly observe the steel core. This indicates that bar 3 was cut from the pointed end of the coppered rod, justifying the delay in the ultrasonic signal, which decreased the results of *VL* and *VT*. Thus, the results of *VL* = 5,872 m/s and *VT* = 3,230 m/s for copper bars were admitted in this study.

Figure 3.1 – Cross-section of the bars: (a) ends used for ultrasound emission and (b) for ultrasound reception, highlighting the copper layer on the face of bar 3

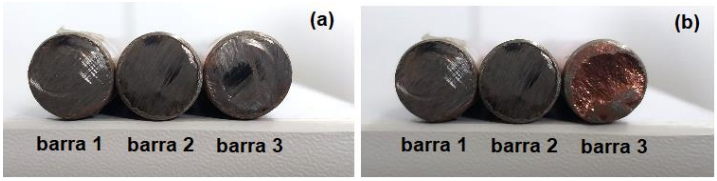

Source: authors (2024)

Gur and Keles (2003) found the following reference values for 1020 steel with ultrasonic waves: *VL* = 5,899 m/s and *VT* = 3,237 m/s. These values also agree with the information in the Olympus technical catalog (2010, p. 49), which adopts VL = 5,890 m/s and *VT* = 3,240 m/s values for 1020 steel. it is noted that the calculated results of *VL* and *VT* for the bars are close to the values reported in the literature for 1020 steel.

Table 3.3 shows the results of *VL* and *VT* after the chemical attack. The chemical attack does not influence the propagation of the ultrasonic signal, and the same values are found with the removal and repositioning of the transducers on the bars. This fact reinforces the hypothesis that the longer propagation time found in bar 3 (Table 3.2) is in fact associated with the presence of the copper layer at one of the ends.

Table 3.3 – *VL* and *VT results* obtained after chemical attack

Bar	Time (hours)	*VL* (m/s)	*VT* = 0,55.*VL* (m/s)
1	24	5,872 ± 0.1	3,230 ± 0.1
2	48	5,872 ± 0.1	3,230 ± 0.1
3	144	5,872 ± 0.1	3,230 ± 0.1
Average	-	5,872 ± 0.1	3,230 ± 0.1

Source: authors (2024)

ELASTIC AND PHYSICAL PROPERTIES OF BARS

Table 3.4 shows the results obtained for the modulus of elasticity with the flexure test. The mean stem deflection calculated with three measurements was 4.00 ± 0.10 mm. Inserting the data from the table into Equation 2.12 showed an approximate result of E = 200.30 ± 5.47 GPa. Some authors report that steels present a proportionality between the applied stress and the strain observed in the tensile and flexural tests (CALLISTER JR, 2012, p. 103; GARCIA; SPIM; SANTOS, 2012, p. 11, 173). In Hooke's Law, the modulus of elasticity is the constant that represents this proportionality and that provides important information about the stiffness of steel.

Table 3.4 – Experimental data for the calculation of the modulus of elasticity

Measurement	*E* (GPa)	*Δ* (mm)	*P* (N)	*L* (mm)	*I* (mm4)
1	203,46	4,10	28,63	1150,00	1087,44
2	203,46	4,10			
3	193,98	4,00			
Mean ± Deviation	200,30 ± 5,47	4.07 ± 0.06			

Source: authors (2024)

For Callister Jr. (2012, p. 642), the modulus E adopted for carbon steel is 207 GPa. Therefore, it is noted that the result found with the flexure test (E = 203.30 GPa) agrees with the reference value adopted for 1020 steel. Freitas et al. (2010) used the ultrasound assay on 1020 steel and found values of the E modulus ranging from 210 to 212 GPa. Using the mean values of VL = 5,872 m/s, VT = 3,230 m/s and = 7,898 ± 16 kg/m³, obtained before the chemical attack of the bars, an approximate result of ρE = 211.45 GPa was found (Table 3.5). This result is in accordance with the value obtained in the flexure test and also with the reference values for 1020 steel.

Table 3.5 – Tensile properties for the bars before chemical attack

Property	Calculated result	Reference values
E (GPa)	211,45	207-212
G (GPa)	82,40	80-82
B (GPa)	162,46	160-163
v	0,28	0,28 - 0,33
A0	0,95	0,90 -1,20

Source: authors (2024)

Table 3.5 also shows other elastic properties calculated before the chemical attack of the bars. Among these properties, the G-modulus stands out for being important for the analysis of the elastic behavior of steel bars when mechanically requested by the cross-section (GARCIA; SPIM; SANTOS, 2012, p. 19). For some authors, the value of the G-modulus in 1020 steel is 80 GPa (DEWANGAN et al., 2019). This reference value is compatible with the result of 82.10 GPa found in 1020 steel with the industrial ultrasound test (FREITAS *et al.,* 2010). Carvalho Jr *et al*. (2021) investigated normalized 1020 steel with ultrasonic waves and found a value of G = 81.68 GPa. Therefore, the calculated result of G = 82.40 GPa is within the range of expected values for 1020 steel.

Modulus B is a property that is directly related to the elastic moduli E and G, representing the stiffness to volumetric deformation of steel (GARCIA; SPIM; SANTOS, 2012, p. 19). In general, the adopted value of modulus B for low-carbon steels is between 160 and 163.10 GPa (FUKUHARA; SANPEI, 1993; KIM; JOHNSON, 2007). In this case, the calculated result of B = 162.46 GPa is also within the range of values reported in the literature.

The v coefficient is a property used to establish the relationship between longitudinal and transverse deformations in isotropic materials. For most carbon steel alloys, v = 0.30 is adopted (CALLISTER JR., 2012, p. 645). On the other hand, the coefficient v of steels measured at room temperature of 25°C can vary between 0.28 and 0.33 (FUKUHARA; SANPEI, 1993; KALPAKJIAN; SCHMID, 2009, p. 86). Thus, the calculated result of v = 0.28 is in line with what is expected for most carbon steels.

In materials considered perfectly isotropic, an anisotropy value is adopted A_0 = 1 (GARCIA; SPIM; SANTOS, 2012, p. 46). In the present study, the result calculated for the bars was A_0 = 0.95. This result confirms the isotropic trends of carbon steel observed by Kalpakjian and Schmid (2009, p. 409). These authors also point out that steels with low carbon content and high tensile strength can present values between 0.90 and 1.20.A_0

As previously discussed, chemical attack with HNO3 did not alter the calculated *VL* and *VT* results, although copper layer removal decreased the density from 7,898 kg/m3 to 7,856 kg/m3.

Thus, the influence of chemical attack on elastic properties can be analyzed by comparing the results in Table 3.6. In general, there are small reductions in the elastic modulus (*E*, *G* and *B*), which still remained within the range of values expected for carbon steels. On the other hand, the results of v and *A0* remained unchanged.

Table 3.6 – Elastic properties of bars before and after chemical attack

Property	Before	After
E (GPa)	211,45	210,32
G (GPa)	82,40	81,96
B (GPa)	162,46	161,60
v	0,28	0,28
A0	0,95	0,95

Source: authors (2024)

Removing the copper layer also reduced the acoustic impedance (*Z*). This physical property can be understood as a difficulty that steel offers to the propagation of ultrasonic waves, being dependent on the stiffness of the material (KRAUTKRAMER; KRAUTKRAMER, 1990, p. 23). As the chemical attack caused small reductions in the results of the elastic modulus associated with the stiffness of the steel (*E*, *G* and *B*), a small change in the result of Z was also expected, as shown in Table 3.7. The results found, before and after the chemical attack, are close to the reference value of *Z* = 45.56 x 106 kg/m2s, reported by other authors who used the ultrasonic transmission method in 1020 steel (GINZEL; TURNBULL, 2016).

Table 3.7 – Elastic properties before and after chemical attack

Property	Before	After	Reference value
Z (106 kg/m2s)	46,380	46,130	45,560
R (10^{-7} Ω.m)	0,083	0,168	0,160

Source: authors (2024)

On the other hand, the electrical resistivity measured after the chemical attack increased significantly, from *R* = 0.083 x 10-7 Ω.m to *R* = 0.168 x 10-7 Ω.m. In the present study, the result of *R* represents the opposition to the flow of the electric energy current through the steel (CALLISTER JR., 2012, pp. 490, 491). It is important to note that the copper coating is intended to protect the grounding rods against corrosion and also to direct any electric current that may damage the equipment to the ground. According to Callister Jr. (2012, p. 661), the electrical resistivity of electrolytic copper is very low, being in the order of *R* = 1.72 x 10-8 Ω.m. Therefore, the removal of

the copper layer increased the resistivity of the bar, in accordance with the reference value of R = 0.160 x 10-7 Ω.m adopted for 1020 steel (CALLISTER JR. 2012, p. 660).

CONCLUSION

The results of this study allowed us to conclude that the electronic ultrasound system can be used to determine elastic and physical properties of copper-coated steel grounding rods. This statement is based on the results found for the modulus of elasticity (E), shear (G) and compressibility (B); Poisson coefficient (v), anisotropy factor (), acoustic impedance (A_0Z) and electrical resistivity (R), whose results calculated with the equations for isotropic materials described as a function of VL, VT and , were compatible with the reference values adopted in the literature for 1020 steel. However, other studies should be carried out with a larger number of rods seeking to improve the non-destructive methodology and the electronic devices used.ρ

REFERENCES

1. Alazoumi, S. H., Sidek, H. A. A., Halimah, M. K., Matori, K. A., Zaid, M. H. M., & Abdulbaset, A. A. (2017). Synthesis and elastic properties of ternary ZnO-PbO-TeO_2 glasses. *Chalcogenide Letters, 14*(8), 303–320. Disponível em: http://www.chalcogen.ro/303_AlazoumiSH.pdf. Acesso em: 04/09/2024.

2. Associação Brasileira de Normas Técnicas. (2008). *NBR 5410: Instalações elétricas de baixa tensão*. Rio de Janeiro.

3. Associação Brasileira de Normas Técnicas. (2024). *NBR 13571: Haste de aterramento de aço revestida de cobre – Especificação*. Rio de Janeiro.

4. ASTM E494-95. (1995). *Standard practice for measuring velocity in materials*. ASTM International, Pennsylvania.

5. Budi, A. S., Hussin, R., & Sahar, M. R. (2002). Study of fractal bond connectivity of neodymium phosphate glasses by ultrasonic technique. *Jurnal Teknologi, 37*, 11–20. Disponível em: https://dx.doi.org/10.11113/jt.v37.529. Acesso em: 04/09/2024.

6. Callister Jr, W. D. (2012). *Ciência e engenharia dos materiais: Uma introdução* (7ª ed.). Rio de Janeiro: LTC.

7. Carvalho Jr, Á. B., Inácio, M. J., Dias, M. P. A., Lopes, M. H. T., Carvalho, A. C. N. M., & Ramos, S. G. (2021). Caracterização das propriedades elásticas e mecânicas do aço 1020 com a técnica ultrassônica da transparência. *International Journal of Advanced Engineering Research and Science (IJAERS), 8*(10), 227–234. Disponível em: https://dx.doi.org/10.22161/ijaers.810.26. Acesso em: 01/09/2024.

8. Carvalho Jr, Á. B., Lopes, M. H. T., Inácio, M. J., Ramos, S. G., Rodrigues, D. S., Froes, G. D., Fonseca, V. M. B., & Oliveira, J. A. V. (2022). Determination of elastic and mechanical properties in CA-50 steel by using ultrasonic. *International Journal of Advanced Engineering Research and Science (IJAERS), 9*(9), 249–255. Disponível em: https://dx.doi.org/10.22161/ijaers.99.25. Acesso em: 02/09/2024.

9. Dewangan, S., Mainwal, N., Khandelwal, M., & Jadhav, P. S. (2019). Performance analysis of heat treated AISI 1020 steel samples on the basis of various destructive mechanical testing and microstructural behaviour. *Australian Journal of Mechanical Engineering, 20*(1), 74–87. Disponível em: https://doi.org/10.1080/14484846.2019.1664212. Acesso em: 02/09/2024.

10. Eraiah, B., Geetha, D., & Anavekar, R. V. (2008). Elastic properties of lead-phosphate glasses doped with erbium trioxide. *Canadian Journal of Physics, 86*(11), 1349–1352. Disponível em: https://doi.org/10.1139/p08-10. Acesso em: 02/09/2024.

11. Eun, T. J. (2020). *Handbook of engineering practice of materials and corrosion* (1ª ed.). Houston: Springer.

12. Freitas, V. L. D. A., Albuquerque, V. H. C. D., Silva, E. D. M., Silva, A. A., & Tavares, J. M. R. S. (2010). Nondestructive characterization of microstructures and determination of elastic properties in plain carbon steel using ultrasonic measurements. *Materials Science and Engineering A, 527*, 4431–4437. Disponível em: https://doi.org/10.1016/j.msea.2010.03.090. Acesso em: 02/09/2024.

13. Fukuhara, M., & Sanpei, A. (1993). Elastic moduli and internal friction of low carbon and stainless steels as a function of temperature. *ISIJ International, 33*(4), 508–512. Disponível em: https://doi.org/10.2355/isijinternational.33.508. Acesso em: 04/09/2024.

14. Garcia, A., Spim, J. A., & Santos, C. A. (2012). *Ensaios dos materiais* (2ª ed.). Rio de Janeiro: LTC.

15. Ginzel, E., & Turnbull, B. (2016). Determining approximate acoustic properties of materials. *e-Journal of Nondestructive Testing (NDT)*, 1–10. Disponível em: https://www.ndt.net/article/ndtnet/2016/17_Ginzel.pdf. Acesso em: 04/09/2024.

16. Gur, C. H., & Keleş, Y. (2003). Ultrasonic characterisation of hot-rolled and heat-treated plain carbon steels. *Insight-Non-Destructive Testing and Condition Monitoring, 45*(9), 615–620. Disponível em: https://doi.org/10.1784/insi.45.9.615.52936. Acesso em: 04/09/2024.

17. Kalpakjian, S., & Schmid, S. R. (2009). *Manufacturing engineering and technology* (6ª ed.). Upper Saddle River: Prentice Hall.

18. Kim, S. A., & Johnson, W. L. (2007). Elastic constants and internal friction of martensitic steel, ferritic-pearlitic steel, and α-iron. *Materials Science and Engineering: A, 452-453*, 633–639. Disponível em: https://doi.org/10.1016/j.msea.2006.11.147. Acesso em: 03/09/2024.

19. Krautkrämer, J., & Krautkrämer, H. (1990). *Ultrasonic testing of materials* (4ª ed.). Berlin: Springer.

20. Lopes, M. H. T., de Carvalho Jr, Á. B., Inácio, M. J., Gomes, S. C. S., Guimarães, T. C., & da Fonseca Jr, A. S. (2024). Utilização de ondas ultrassônicas para caracterização não destrutiva de vergalhões de aço com diferentes tratamentos térmicos. *Contribuciones a Las Ciencias Sociales, 17*(6), 1–15. Disponível em: https://dx.doi.org/10.55905/revconv.17n.6-221. Acesso em: 03/09/2024.

21. Meza, C. A., Franco, E. E., & Ealo, J. L. (2019). Implementation of the ultrasonic through-transmission technique for the elastic characterization of fiber-reinforced laminated composite. *Dyna, 86*(208), 153–161. Disponível em: https://doi.org/10.15446/dyna.v86n208.70279. Acesso em: 03/09/2024.

22. Olympus. (2010). *Panametrics – Ultrasonic transducers*. Disponível em: https://www.olympus-ims.com/data/File/panametrics/panametrics-UT.en.pdf. Acesso em: 03/09/2024.

23. Palani, R., & Selvarasi, J. (2017). Elastic and structural properties of potassium and calcium-doped borate lithium glasses. *International Journal of Current Research and Review (IJCRR), 9*, 71–79. Disponível em: https://ijcrr.com/uploads/1145_pdf.pdf. Acesso em: 03/09/2024.

24. Waag, G., Hoff, L., & Norli, P. (2012). Air-coupled thickness measurements of stainless steel. *ArXiv preprint arXiv:1210.0428, 1*(1), 1–4. Disponível em: https://doi.org/10.48550/arXiv.1210.0428. Acesso em: 04/09/2024.